Hindawi
Scientific Programming
Volume 2023, Article ID 9816825, 1 page
https://doi.org/10.1155/2023/9816825

Retraction

Retracted: Application of Three-Dimensional Image Reconstruction Technology in Neurogenic Intestinal Nursing Tasks

Scientific Programming

Received 26 September 2023; Accepted 26 September 2023; Published 27 September 2023

This article has been retracted by Hindawi following an investigation undertaken by the publisher [1]. This investigation has uncovered evidence of one or more of the following indicators of systematic manipulation of the publication process:

(1) Discrepancies in scope
(2) Discrepancies in the description of the research reported
(3) Discrepancies between the availability of data and the research described
(4) Inappropriate citations
(5) Incoherent, meaningless and/or irrelevant content included in the article
(6) Peer-review manipulation

The presence of these indicators undermines our confidence in the integrity of the article's content and we cannot, therefore, vouch for its reliability. Please note that this notice is intended solely to alert readers that the content of this article is unreliable. We have not investigated whether authors were aware of or involved in the systematic manipulation of the publication process.

Wiley and Hindawi regrets that the usual quality checks did not identify these issues before publication and have since put additional measures in place to safeguard research integrity.

We wish to credit our own Research Integrity and Research Publishing teams and anonymous and named external researchers and research integrity experts for contributing to this investigation.

The corresponding author, as the representative of all authors, has been given the opportunity to register their agreement or disagreement to this retraction. We have kept a record of any response received.

References

[1] Y. Shen, X. Huang, Y. Zhang, J. Pan, Y. Liu, and Y. Jiang, "Application of Three-Dimensional Image Reconstruction Technology in Neurogenic Intestinal Nursing Tasks," *Scientific Programming*, vol. 2022, Article ID 4840189, 10 pages, 2022.

Hindawi
Scientific Programming
Volume 2022, Article ID 4840189, 10 pages
https://doi.org/10.1155/2022/4840189

Research Article

Application of Three-Dimensional Image Reconstruction Technology in Neurogenic Intestinal Nursing Tasks

Yinli Shen,[1,2] Xiaoxing Huang,[1] Yue Zhang,[1] Jing Pan,[1] Yaxin Liu,[1] and Yunlan Jiang [1,2]

[1]*Chengdu University of Traditional Chinese Medicine, Sichuan, Chengdu 610075, China*
[2]*Hospital of Chengdu University of Traditional Chinese Medicine, Sichuan, Chengdu 610072, China*

Correspondence should be addressed to Yunlan Jiang; b20161001418@stu.ccsu.edu.cn

Received 25 August 2022; Revised 19 September 2022; Accepted 24 September 2022; Published 11 October 2022

Academic Editor: Lianhui Li

Neurogenic intestinal care is currently a major research topic in the medical field. In order to improve the accuracy of neurogenic intestinal care and simplify the process of neurogenic intestinal care, this paper adopts a three-dimensional analysis theory to extract the key indicators in neurogenic intestinal care. Through the analysis and calculation of the test data, the calculation results of neurogenic intestinal care under the effect of three-dimensional reconstruction technology were obtained. Through the analysis of the results, the calculation law under the action of the optimization model can be obtained. Based on the three-dimensional reconstruction theory, the contents of neurogenic intestinal care were analyzed by the three-dimensional reconstruction dehighlighting algorithm. The three-dimensional curve was used to screen the key indicators of neurogenic intestinal care, so as to obtain the optimized heavy weight model, and the three-dimensional reconstruction model can analyze the indicators of neurogenic intestinal care. It can be seen from relevant studies that different indicators have different trends in their range of change in the curve projection diagram of the 3D curve screening method. Among them, the curve shadow and curve point have obvious downward changes, while the curve deviation has *U*-shaped changes. The range of curve weights is relatively large. The variation rule between different data in the 3D curve segment can be obtained through the cost function. Among them, the cost function index and the cost model parameter have the same change trend, and the overall fluctuation range is relatively small through the space index. In the calculation results of neurogenic intestinal care, different factors will have a great influence on the calculation results. Neurons and intestinal peristalsis have the same change trend, while the linear characteristics of nerve endings are relatively obvious, and the fluctuation characteristics of gastrointestinal digestion are good. The health standard decreases linearly with the increase of the sample, and the dynamic reconstruction has a positive effect on the data. This study can provide research ideas for the analysis of neurogenic gut.

1. Introduction

The 3D reconstruction theory was based on the image analysis of relevant data and feature values by using 3D technology. By using the method of image analysis, the relevant indicators can be reconstructed in three dimensions, so as to obtain the original state and change process of the sample. Using this method, the original process of the sample can be analyzed, and the corresponding change characteristics and indexes can be obtained. The 3D image reconstruction theory plays a typical role in different professional fields. Related fields mainly include medical surgery [1], model reconstruction [2], ultrasound propagation [3], three-dimensional pixels [4], etc. In the field of medical donor image reconstruction, the existing medical donor image reconstruction needs a large amount of data, and the data cannot better reflect the original shape of the medical donor, there were some problems such as poor accuracy. Based on the three-dimensional reconstruction theory [5], the data analysis method was used to describe the medical donor image, and the description was combined from the local and the whole, so as to obtain the accurate model calculation results. The results of the model can reflect the real situation of the medical donor image to a certain extent, which can provide accurate guidance for the research in the field of medical workers.

Facial contour reconstruction was very important to improve facial recognition. The existing facial contour reconstruction techniques still remain in the qualitative research, and the research on the real situation of the face was relatively poor. Based on the 3D model reconstruction technology [6], the method of data iterative analysis was used to calculate the facial contour iteratively. This method can not only show the variation characteristics of facial contour but also reflect the volatility of specific data to a certain extent, which can better reflect the technical characteristics of facial contour reconstruction. Facial contour reconstruction technology was very important to improve the recognition of facial contour. In order to verify the accuracy of the model, the experimental data and facial contour recognition parameters were compared to illustrate the accuracy of the experimental results, which reflects the broad application prospect of facial contour recognition technology. In the field of visual communication, the existing visual communication efficiency was low, which cannot reflect the real visual communication characteristics of samples. Based on the three-dimensional reconstruction technology [7], the method of neural network iterative calculation was used to optimize the existing visual transmission model. The optimization model mainly iterates on specific parameters, so as to find the optimal parameters and bring the parameters into the model, so as to obtain the visual communication optimization model based on three-dimensional reconstruction technology. The experimental verification can better illustrate the accuracy of the experimental model, which can provide a theoretical basis for the study of visual communication. The low resolution of the model grid was the main factor that disturbs the model grid, and also restricts the popularization of the model grid. Based on the 3D reconstruction technology [8], the data feature simulation method was used to optimize the mesh resolution. The optimization method mainly performs iterative analysis on the corresponding data, so as to find the optimal iterative data. The iterative data were brought back to the grid resolution model to obtain the corresponding optimized grid resolution model. The model can well and accurately explain the changing process of mesh resolution, so as to carry out targeted analysis. The research can provide guidance for mesh resolution.

The abovementioned studies mainly analyzed the application of 3D reconstruction technology from the fields of grid and visual communication, but there were few studies on the existing problems in neurogenic intestinal care. In this paper, based on three-dimensional reconstruction technology, the de-highlighting algorithm and three-dimensional curve screening analysis method were used to analyze the indicators of neurogenic intestinal care. Through the analysis, the corresponding targeted index can be obtained. Using this targeted index, the change process of divine intestinal care can be better explained, so the corresponding optimization model can be obtained. Through calculation, it can be seen that the optimization model can better reflect the change process of key indicators in neurogenic intestinal care. Finally, the corresponding experimental data can be used to verify the accuracy of the model, which can provide support for neurogenic intestinal care.

2. Three-Dimensional Reconstruction Theory

Image quality is the basis of image algorithm, and the quality of image directly affects the effect of the algorithm [9, 10]. Before the implementation of image correlation algorithm, it is necessary to preprocess the image to suppress the useless information in the image and enhance the relevant information of the tested object [11, 12]. First, the number and initial position of the key points of the 3D model were determined according to the segmented 3D point cloud of the catheter center line. Second, the least square method is used to iteratively fit the 3D point cloud model and the initial key point line segment. Finally, the key converges to the stable optimal value to obtain the most accurate coordinate of the key point.

The 3D image reconstruction system plays an important role in many fields [13, 14]. To successfully apply it to neurogenic intestinal care, the flowchart of 3D reconstruction system as shown in Figure 1 was obtained through summary analysis. It can be seen from the figure that the 3D reconstruction system can be divided into three parts: image sequence import, image region segmentation and data processing, which can be shown as follows: In the image sequence processing module, the basic 3D image is linearized first; then, the illumination data of the corresponding image are extracted. Through the corresponding de-highlight processing, the corresponding optimized image is obtained; then, it is imported into the image region segmentation module. In the image region segmentation module, the image should be first segmented regionally, and then further refined to obtain the corresponding center line branch line through image refinement. The corresponding optimization data are obtained by segmentation and then imported into the data architecture module. In the data processing module, the center line of the space should be reconstructed first. Through the reconstruction of the center line of the space, the corresponding center line data can be obtained, and the data can be spliced. The fitting equation of 3D image data is obtained by data stitching, and the final calculation and measurement are carried out; then, the corresponding processing data are exported. First, the polar lines in adjacent images are calculated for a set of 2D curve segments of each data, and the matching points are found through the polar line geometry to generate the candidate 3D curve segments of each set of 2D curve segments. Second, the global selection problem is solved to select the most correct set of 3D curve segments from the candidate set.

2.1. 3D Image De-Highlighting Algorithm. First, the centerline coordinates of the catheter plane image were extracted, and the candidate three-dimensional curve segment set was generated according to the stereo vision principle. Second, the global selection problem is solved to select a 3D curve from the candidate set. Finally, the optimal path

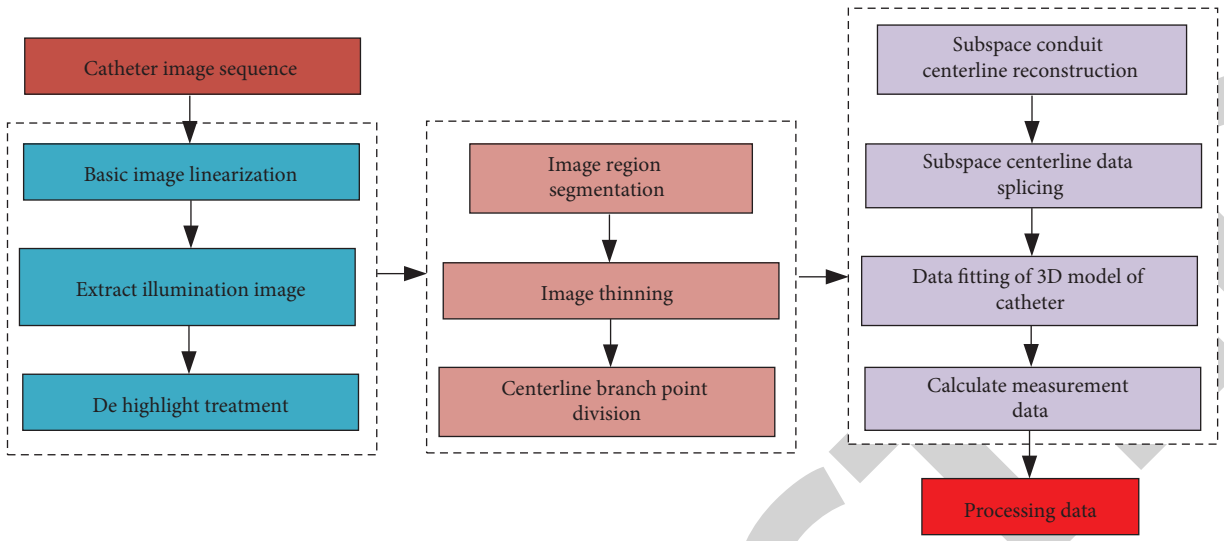

Figure 1: Technical route of the 3D image reconstruction system.

reconstruction catheter 3D model is found. Aiming at the phenomenon of surface highlight reflection produced by 3D reconstruction technology under intestinal care, this section adopts a highlight removal algorithm based on 2D gamma function image [15, 16]. First, the luminance component v in the channel of neurogenic intestine was extracted, and the illumination component was extracted by multiscale Gaussian blur. Second, the 2D gamma function is used to adjust the brightness component of the original image, and the highlight image is corrected on the premise of effectively retaining the effective information of the original image [17, 18]. By recovering the global topological structure of the three-dimensional curve segment, the subspace three-dimensional curve segment of the binocular system was data concatenated to find the optimal path to reconstruct the complete three-dimensional model of the catheter centerline. To solve the problem of weak texture and difficult matching of feature points on the surface of the model, the polar geometry method is used for space matching. The specific implementation steps are as follows:

(1) The multiscale Gaussian function is used to extract the illumination component in the image of neurogenic intestine. The Gaussian function form is as follows:

$$G(x, y) = \lambda \exp\left(-\frac{x^2+y^2}{c^2}\right), \tag{1}$$

where c represents the scale proportion and λ represents the normalization constant. By applying Gaussian blur to the original image, multiscale illumination components of the image in the neurogenic intestinal channel were extracted, and the results were as follows:

$$F(x, y) = I(x, y)G(x, y),$$
$$F(x, y) = I(x, y)\lambda \exp\left(-\frac{x^2+y^2}{c^2}\right), \tag{2}$$

where $F(x, y)$ represents the estimated model component, and $I(x, y)$ represents the input original graph.

The corresponding 3D image de-highlighting algorithm can be obtained by 3D reconstruction theory, and the specific image data in intestinal care can be extracted by the multiscale Gaussian function [19, 20]. The corresponding Gaussian change curve can be obtained through analysis, as shown in Figure 2. It can be seen from the curve in the figure that the factors affecting the change of Gaussian mainly include as follows: input original graph, Gaussian function, and corresponding model components. The output results under the action of these three factors have different changing trends, as can be seen in detail: It can be seen from the input curve corresponding to the original figure that with the increase of independent variables, the curve first slowly increases to the local maximum value, and then gradually tends to be flat. With the further improvement of independent variables, the curve gradually fluctuates, and the fluctuation range is relatively small. Then, when the independent variable is at a higher level, the curve gradually decreases and finally tends to be stable. The change trend of the overall input original graph basically fluctuates within a small range, indicating that its influence on the output result is relatively small. With the increase of independent variables, the corresponding curve of Gaussian function decreases first and then gradually tends to be gentle, and then, the curve fluctuates further. When the independent variables are higher, the curve gradually tends to be stable. The overall variation range and variation trend are exactly opposite to the corresponding curve variation trend under the action of factors in the input original graph. This shows that the two have opposite effects on the output results, and it can be seen from the model component change curve that with the

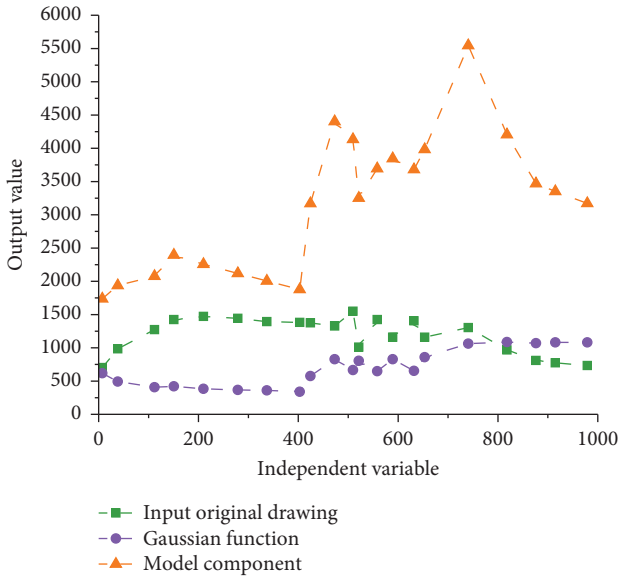

Figure 2: Gaussian change curve.

increase of independent variables, the curve first gradually increases to the local maximum value and then gradually decreases. The amount of decrease in the descending stage of the curve is basically the same, indicating that its linear feature is relatively obvious. Then, when the independent variable is further improved, the curve increases rapidly. Then it is shown that there is a certain jump in the data at this stage, resulting in a large fluctuation of the corresponding output results in a certain range. Then, with the further increase of independent variables, the corresponding output curve shows a trend of greater volatility. The overall fluctuation range of the curve is relatively wide, indicating that it has a great influence on the output result.

(2) Construct the two-dimensional gamma function as shown below and use the two-dimensional gamma function to correct the image of the highlight component and reduce the brightness value of the image of the highlight part.

$$Q(x, y) = 255\left(\frac{F(x, y)}{255}\right)^{\gamma},$$
$$\gamma = (1/2)^{P}, \tag{3}$$
$$P = \frac{I(x, y) - m}{m},$$

where $I(x, y)$ is the input image, $F(x, y)$ is the model component image, $O(x, y)$ is the corrected output image, γ is the index value of image brightness enhancement, and m is the luminance mean value of the illumination component.

By using the multiscale Gaussian function in the theory of 3D image de-highlighting, the corresponding trend map of neurogenic intestinal image processing can be obtained [21, 22]. By constructing a two-dimensional gamma function curve, you can analyze the different parameters in it. Through analysis, it can be seen that the influencing factors of two-dimensional gamma function mainly include input image, model component, output image, incremental index, and corresponding mean function. To illustrate the quantitative analysis of the two-dimensional gamma function curve by these five factors, the variation curve of the two-dimensional gamma function as shown in Figure 3 was obtained by calculation. It can be seen from the curve that the output results under the action of five different factors have different change trends, and their specific data have different change forms. As can be seen from the curve corresponding to the input function, with the increase of samples, the curve firstly linearly increases to the local maximum value and then gradually tends to be gentle and then slowly decreases. The decrease amount is relatively small compared with the first stage. Then, with the further increase of the sample, the curve gradually decreases and then increases again, showing a U-shaped change trend, and the overall range of change is relatively large. It shows that this factor can have a great influence on the calculation result of dependent variable. According to the corresponding curve of the graph component, it can be seen that the curve decreases linearly with the increase of the sample. When it reached the lowest value, the curve showed a trend of gradual improvement with the increase of samples. It can be seen from the change trend that the change range of the first stage is larger than that of the second stage, indicating that the first stage of the curve has a higher impact on the dependent variable. According to the corresponding curve of the output function, when the sample is low, the curve gradually tends to be gentle; when the sample is high, the curve first decreases and then increases and finally gradually tends to be stable. The overall stability of the curve is obvious. This indicates that it has little influence on the dependent variable. According to the curve corresponding to the incremental index, it can be seen that with the increase of samples, the curve first increases rapidly to the highest value. Then the sample increase will lead to the corresponding dependent variable data showing a linear decline, with a relatively small range of decline. When the number of samples is 30, the curve reaches the lowest value, indicating that the corresponding calculation result at this point has the minimum value. Then, with the further increase of samples, the output results of the corresponding dependent variable gradually tend to be stable. The curve has an obvious effect on the dependent variable sample of 12. As can be seen from the mean function, the increase of samples will lead to the linear increase of the corresponding dependent variable. Then, when

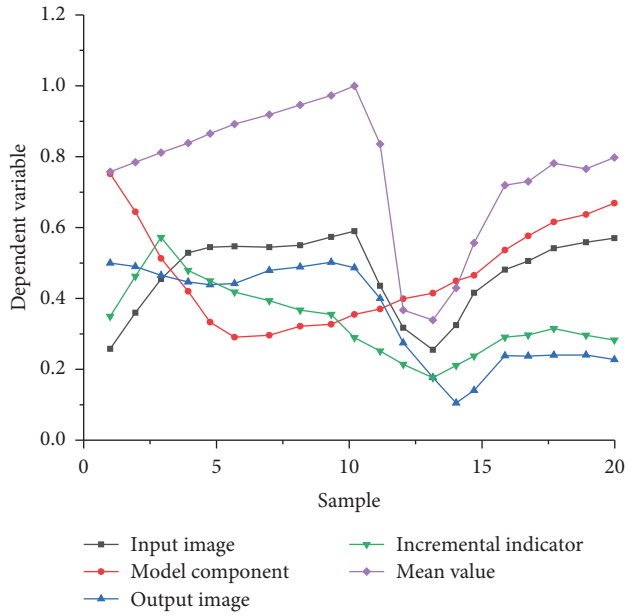

Figure 3: Two-dimensional gamma function graph.

the corresponding sample is gradually improved, the curve decreases first and then increases, showing a *U*-shaped characteristic. The curve shows typical linear characteristics in the first stage, and obvious nonlinear characteristics in the second stage, indicating that the curve corresponding to the mean value function has linear and nonlinear characteristics of common change.

2.2. Three-Dimensional Curve Screening. In the ideal case, there is only one candidate 3D curve segment corresponding to the 2D curve segment of the reference image [23, 24]. If there are multiple candidate 3D curve segments, it is necessary to select a correct curve segment from a set of candidate 3D curve segments by calculating the confidence degree and pairwise cost [25]. The confidence measure measures the matching degree between the 3D candidate curve segment and the curve in the third image, projects each 3D candidate curve segment onto the third image and finds the 2D curve segment in the third image with the smallest projection difference with the candidate curve segment. For the point set, u is the projection on the 3D curve segment, and v is its corresponding point closest to u on the 2D curve segment. The confidence can be calculated as follows:

$$S = \frac{\sum(u, v) + \eta(1 - t)}{s}, \tag{4}$$

where S is confidence degree, s is the sampling point, u is the curve projection, v is the curve point, t is curve deviation, and η is the weight. First, the factors affecting image processing are analyzed, and then, the method of removing highlight of image is introduced in detail, and the light source method used in the measurement system is explained. The influence of light source on image processing quality is also pointed out. Finally, the image is refined and segmented, and the center line of each image is extracted to prepare for 3D reconstruction.

Through the theory of 3D image de-highlighting, the corresponding law of image subdivision calculation can be obtained. To illustrate the role of 3D image reconstruction technology in neurogenic intestinal care, the corresponding curves of 3D images need to be screened to some extent. The curve variation law under the action of different factors was obtained by calculation. To explore the influence of different factors on the projection results in the process of curve projection, the curve projection diagram shown in Figure 4 was obtained through calculation. The influence of different factors on the curve is mainly reflected in the changing shape of the curve. Specifically, it can be seen that: With the increase of the sample points, the curve corresponding to the projection factor shows a gradual decreasing trend. The decline range of the curve in the first stage is relatively small, while the decline range in the second stage is relatively large, indicating that the sampling point has a great impact on the confidence of the data when it is high. As can be seen from the variation law of data points, the curve first increases, then decreases rapidly, and finally gradually tends to be stable, indicating that the curve will gradually tend to be stable under the action of higher sampling points. According to the curve deviation data, it can be seen that with the increase of sampling points, the curve as a whole shows a U-shaped change law. The curve first gradually increases to the highest value, and when the sampling point is about 35, the curve reaches the highest value, and then with the further increase of the sampling point, the corresponding confidence gradually decreases. The overall change in the curve is large in the first period and relatively small in the second period. According to the weight factor of the curve, it can be seen that it shows a typical two-stage change: the inverted U-shaped change range of the curve is relatively small in the first stage. When the corresponding sampling point of the curve is high in the second stage, the curve shows an inverted U-shaped change with a relatively large variation range. The overall variation range of the curve indicates that it has a relatively large impact on the confidence degree. Because of the disparity in the field of view, confidence alone is not enough to describe the matching degree of curve segments to resolve all ambiguities. Therefore, pairwise costs need to be calculated for further screening. Pairwise relation describes the relation between two adjacent three-dimensional candidate curve segments.

Since only one 3D curve segment needs to be selected from each candidate set, a linear constraint for each given is as follows:

$$\sum_{A \in C} X(j) = 1. \tag{5}$$

Next, we define a pairwise relation cost function d to evaluate the pairwise relation between 3D curve segments:

$$\mathrm{dA}A = eA1 + mA2, \tag{6}$$

where e is the space distance; m is the model parameter. The correct 3D curve segment is reconstructed from a curved, continuous conduit object, along which the continuous curve segment is smoothly connected. Therefore, adjacent

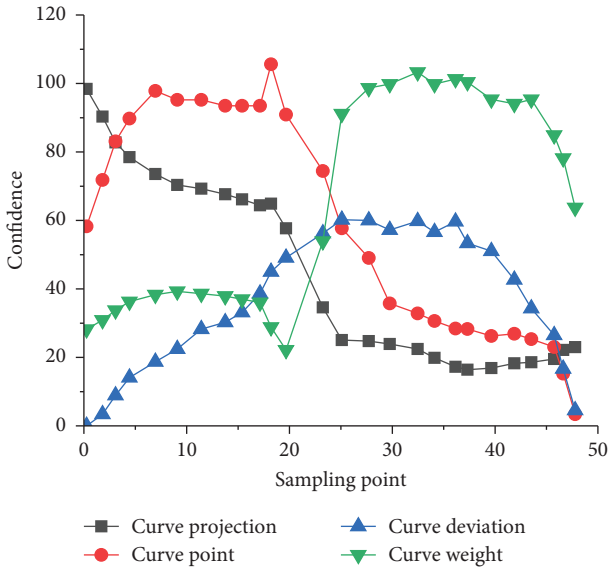

Figure 4: Curve projection diagram.

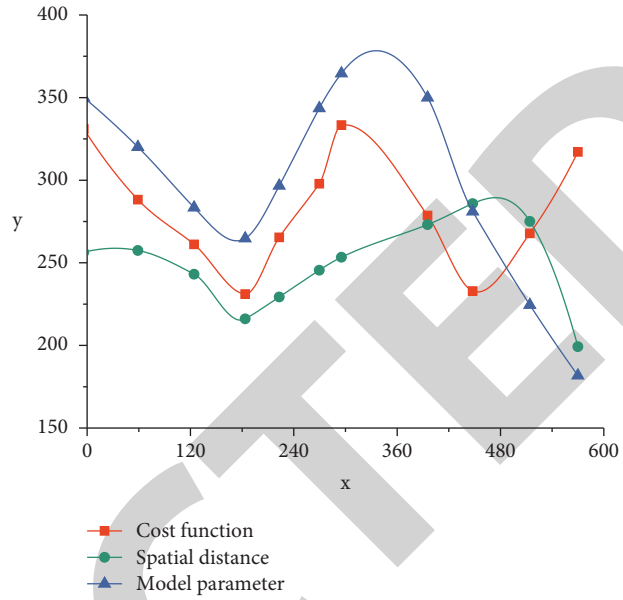

Figure 5: Change of cost function.

3D curve segments with similar angles are more likely to be the correct 3D curve segment, which provides a more effective matching cue to formalize these cues in the optimization problem.

The corresponding linear constraint law can be obtained by selecting 3D curves from different sets. The linear constraint law can reflect the change trend under the action of different cost functions, so as to explain the influence of different factors in the change law of cost functions, and then reflect the corresponding curve screening process and corresponding accurate results. The change trend of the cost function as shown in Figure 5 is obtained through calculation. It can be seen from the figure that the overall fluency of the curve is relatively good. The corresponding output results of the cost function are shown as W-shaped fluctuation changes which first decrease and then increase and then decrease and then increase. The corresponding model parameters also show the same change trend with the increase of independent variables, but under the action of higher independent variables, the curve gradually decreases, contrary to the change trend of the corresponding cost function. However, the corresponding modular space distance decreases first and then increases gradually with the change of the cost function, and the overall change range of the curve is relatively small, indicating that its influence on the output result of the cost function is relatively small.

Finally, the vector U is used to represent the combined confidence scores of all 3D curve segments, and V is the pairwise cost variable, giving U and V, minimizing X as follows:

$$\begin{aligned} X &= \operatorname{argmin}\left(U^T X + X^T \mathrm{VX}\right), \\ \forall C_i^r &= \sum_{A_j = C_i^r} X(j)1, \\ \{\mathrm{xij}\} &= \underset{\{k,\mathrm{xij}\}}{\operatorname{argmin}} \sum_{i,j} \mathrm{xijwij} + \xi k. \end{aligned} \tag{7}$$

Through the above calculation, the quantitative change rule of the cost function under the action of different factors can be obtained. To research the specific changes of confidence in the three-dimensional curve, the direct line parameter analysis diagram shown in Figure 6 is obtained through calculation. It can be seen from the analysis figure that the three factors will have an impact on the output result of the dependent variable of confidence, and the curve under the action of the three factors can be seen that the overall fluctuation range is relatively large. As can be seen from the changes in the figure, with the increase of independent variables, the curve first gradually increases to the highest value and then gradually decreases to the lowest value. However, it can be seen from the cost that the curve is contrary to the confidence degree, that is, the curve gradually decreases to the highest value first and then increases gradually. As can be seen from the minimization factor curve, the curve decreases first and then increases with the increase of the independent variable. The three curves as a whole show fluctuations, and the variation range of the minimization curve is relatively small.

3. Application of Three-Dimensional Image Reconstruction Technology in Neurogenic Intestinal Care

3.1. The Main Content of Neurogenic Intestinal Care. The 3D reconstruction theory can be used to de-highlight the 3D image, so as to obtain the corresponding 3D image screening results. Through the screening results of 3D images, the application model of 3D images in neurogenic intestinal care was obtained by further analysis. First of all, we need to conduct qualitative analysis of neurogenic gut, and the

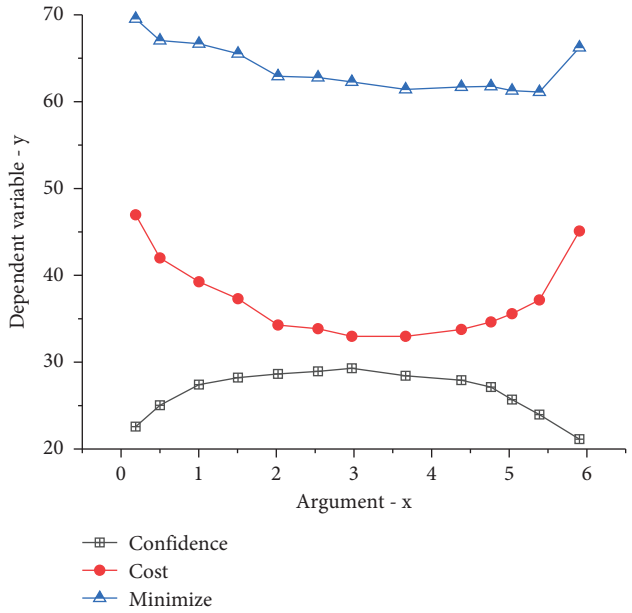

Figure 6: Confidence parameter analysis diagram.

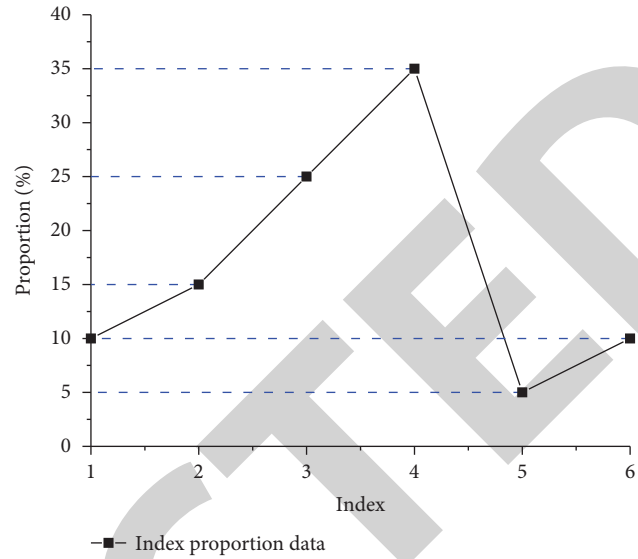

Figure 7: Neurogenic bowel analysis diagram.

corresponding neurogenic gut analysis chart shown in Figure 7 can be obtained by summarizing relevant data. As can be seen from the figure, the proportion of neurons under the action of different factors is different, so it is necessary to carry out targeted analysis. Among them, the proportion of neurons is only 10%, while the proportion of intestinal peristalsis is about 15%. The corresponding nerve terminal factors accounted for about 25%, while the corresponding intestinal digestion accounted for the highest proportion (about 35%), the health standard accounted for the lowest proportion (only 5%), and the dynamic remodeling accounted for about 10%.

3.2. Calculation and Analysis of Three-Dimensional Image Reconstruction Technology in Neurogenic Intestinal Care. There are many problems in the nursing of neurogenic intestines. To better solve the problem of low accuracy in the nursing of neurogenic intestines. In this paper, the 3D reconstruction technology is used to de-highlight the related images and screen the curves, so as to get the corresponding 3D image reconstruction model. This model can quantitatively analyze neurogenic intestines. To better illustrate the analysis process of 3D image reconstruction technology, the 3D image reconstruction analysis flowchart shown in Figure 8 is obtained by summarizing. Through the model analysis process, it can be seen that: first, graphic modeling should be carried out for 3D reconstruction technology, and the corresponding cloud generated graph should be obtained through graphic modeling. The corresponding gastrointestinal model was obtained by correcting the model. The gastrointestinal model can be calculated in the process of model cloud import, and then, the corresponding neurogenic intestinal model can be obtained. The neuronal model is mainly completed by 3D modeling in the aspect of intestinal data collection, and then, the model needs to be adjusted on the basis of this model. The adjustment of 3D neurogenic intestinal model mainly includes model angle, model position, model data, and model indicators. Finally, it is visualized, and the final output result is obtained through model effect rendering. To solve the accuracy problem in 3D reconstruction, the 3D curve segments were divided by the number of intersection points of the polar lines and several candidate 3D curve segments were reconstructed. By reprojecting the candidate 3D curve segments, the 3D curve segment with the minimum projection difference was selected to improve the accuracy of catheter centerline reconstruction.

The abovementioned calculation process can be used to de-highlight the 3D image model and screen the 3D curve, so as to obtain the application of 3D image reconstruction technology in neurogenic intestinal care. The calculation results of neurogenic intestinal care were obtained as shown in Figure 9. Through the calculation results, we can see the overall change trend of different factors under the action of neurogenesis. Specifically, it can be seen that with the increase of samples, neurons show a change of first decreasing, then increasing, and then decreasing. The overall fluctuation range of the curve is relatively obvious, but the fluctuation range is relatively small. As can be seen from the curve of intestinal peristalsis, it is basically consistent with the overall change trend of neurons, that is, the curve decreases first and then increases. However, it is worth noting that the data of the intestinal peristalsis curve are larger than that of the neuron curve, indicating that its influence on intestinal care is relatively extensive. According to the corresponding curve of nerve endings, it can be seen that the curve increases first and then decreases, and the overall decline is relatively obvious, indicating that it has a negative impact on data output. According to the gastrointestinal digestion curve, it can be seen that the curve will fluctuate to a certain extent under the action of small samples, and then gradually tends to be stable under the action of high samples, indicating that different samples will have different effects on the data

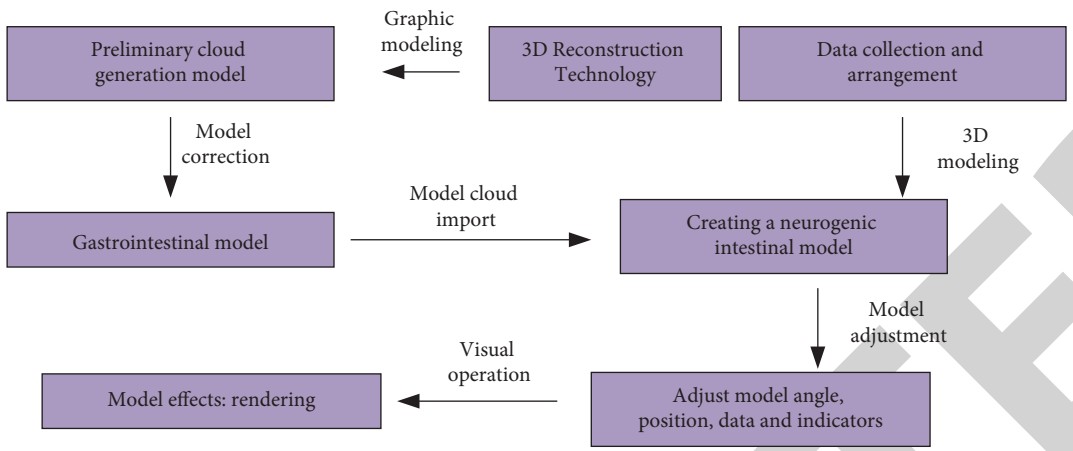

Figure 8: Analysis flowchart of 3D image reconstruction technology.

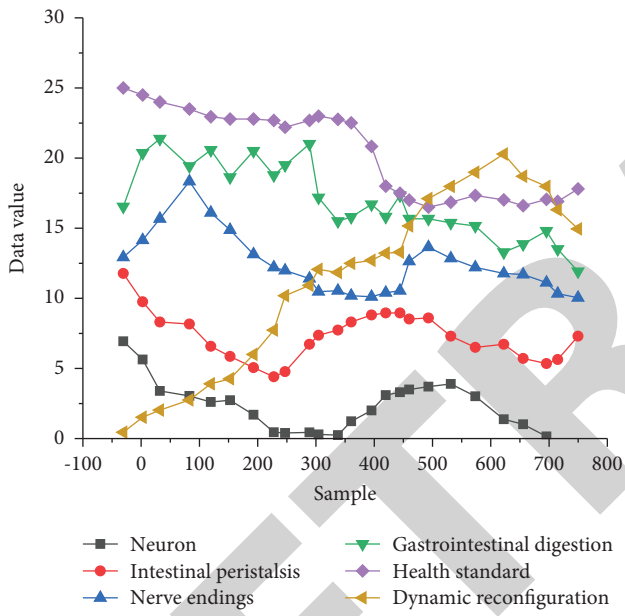

Figure 9: Calculation results of neurogenic intestinal care.

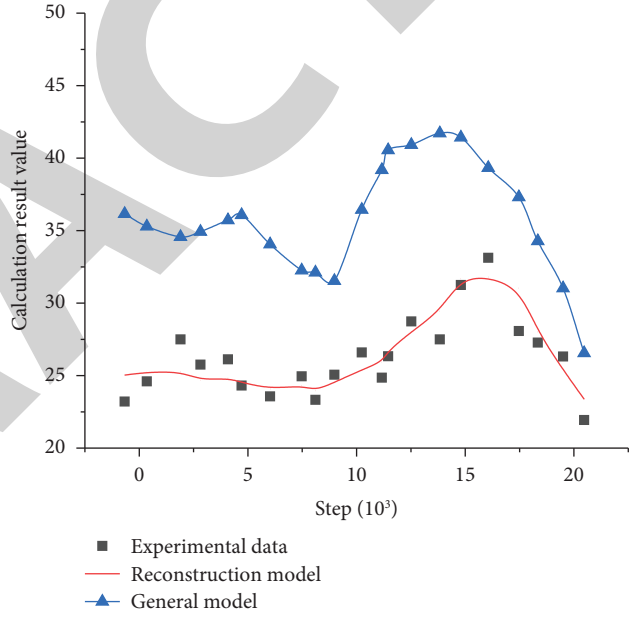

Figure 10: Model validation curve.

results of gastrointestinal digestion. It can be seen from the health standard that the curve corresponding to the health index gradually tends to be stable with the increase of the sample and then decreases rapidly when the sample is about 400, and then gradually tends to be stable. The overall range of change is relatively small, and the curve has good stability. Through dynamic reconstruction, it can be seen that the curve shows a gradual improvement trend under the action of small samples, and the overall linear range is relatively obvious. When it reaches the highest level, the curve gradually decreases with the increase of samples. It shows that it has a certain volatility to the sample data, and the overall linear characteristics are relatively obvious, indicating that it has a positive impact on the data value. The goal is to find multiple different paths that start and end with constant lengths such that each data is contained in exactly one path. Each of these paths corresponds to a continuous 3D line of the conduit model, and each path is uniquely determined by the edges it is composed of. The path finding problem is solved by minimizing the objective function.

4. Discussion

Based on the 3D reconstruction theory, the 3D image dehighlighting algorithm and 3D curve screening method were used to obtain the application of 3D image reconstruction technology in neurogenic intestinal care, and the corresponding optimization model was obtained through calculation. This optimization model can calculate the data of neurogenic intestine at different moments for accurate analysis. To quantitatively illustrate the accuracy of the model curve, the curve calculation results under the action of different models are obtained through calculation, as shown in Figure 10. It can be seen from the results that the corresponding test data gradually increases with a small number of iterations and then gradually decreases. The overall

volatility of the curve is relatively model. Through the conventional model curve, it can be seen that the curve decreases first and then increases with the increase of the number of iteration steps. The overall trend of change can well explain the experimental data, but there are great differences in specific values. Through the reconstruction curve, it can be seen that the curve can not only well illustrate the trend of the data at lower iterations but also the trend of the data and the trend of the curve at higher iterations. It shows that the reconstructed model has good accuracy. At the same time, it also shows that three-dimensional reconstruction technology has a good application in neurogenic intestinal care.

5. Conclusion

(1) According to the Gaussian change curve in the 3D image de-highlighting algorithm, it can be seen that the input original image and Gaussian function have the opposite change trend. On the other hand, the component curve of the model changes significantly with the increase of independent variables, indicating that it has a high impact on the output results.

(2) Five different factors will have different effects on the two-dimensional gamma function, among which the input function model component and the output function have the same changing trend. The corresponding incremental index fluctuates within a small range of change, and the overall linear and nonlinear characteristics are obvious through the mean value.

(3) In the confidence analysis curve, the confidence parameter shows an inverted *U*-shaped change, and the curve corresponding to the cost index shows an opposite *U*-shaped change. The trend of the minimum value shows that its influence on the dependent variable is relatively small, and the stability of the curve is relatively good.

Data Availability

The data used to support the findings of this study are available from the corresponding author upon request.

Conflicts of Interest

The author declare that they have no known conflicts financial interests or personal relationships that could have appeared to influence the work reported in this paper.

References

[1] M. Chen, N. Xia, and Q. Dong, "The application of 3D technology combined with image navigation in nasal skull base surgery," *Journal of Craniofacial Surgery*, vol. 125, no. 60, pp. 630–652, 2020.

[2] D. Jeong, Y. Li, H. J. Lee et al., "Efficient 3D volume reconstruction from a point cloud using a phase-field method," *Mathematical Problems in Engineering*, vol. 28, no. 10, pp. 1–9, 2018.

[3] J. Dong, W. Cong, D. Ai et al., "Multi-resolution cube propagation for 3D ultrasound image reconstruction," *IEEE Transactions on Computational Imaging*, vol. 12, no. 2, pp. 1–15, 2019.

[4] M. Li, A. Mathai, L. Yandi, Q. Chen, X. Wang, and X. Xu, "A brief review on 2D and 3D image reconstruction using single-pixel imaging," *Laser Physics*, vol. 30, no. 9, pp. 095204–095267, 2020.

[5] I. Maamoun and M. M. Khalil,"Assessment of iterative image reconstruction on kidney and liver donors: potential role of adaptive iterative dose reduction 3D (AIDR 3D) technology," *European Journal of Radiology*, vol. 109, no. 110, pp. 120–145, 2018.

[6] Y. Wang, N. Deng, and B. Xin, "Investigation of 3D surface profile reconstruction technology for automatic evaluation of fabric smoothness appearance," *Measurement*, vol. 166, no. 23, pp. 108264–109124, 2020.

[7] J. Yin and J. H. Yang, "Virtual reconstruction method of regional 3D image based on visual transmission effect," *Complexity*, vol. 20, no. 12, pp. 20–30, 2021.

[8] H. Zhang, Y. Shinomiya, and S. Yoshida, "3D MRI reconstruction based on 2D generative adversarial network super-resolution," *Sensors*, vol. 21, no. 9, pp. 536–549, 2021.

[9] A. D. Speers, B. Ma, W. R. Jarnagin, S. Himidan, A. L. Simpson, and R. P. Wildes, "Fast and accurate vision-based stereo reconstruction and motion estimation for image-guided liver surgery," *Healthcare Technology Letters*, vol. 5, no. 20, pp. 208–214, 2018.

[10] F. Chen, K. Muhammad, and S. H. Wang, "Three-dimensional reconstruction of CT image features based on multi-threaded deep learning calculation," *Pattern Recognition Letters*, vol. 136, no. 52, pp. 756–782, 2020.

[11] L. Deng and Y. Pu, "Analysis of college martial arts teaching posture based on 3D image reconstruction and wavelet transform," *Displays*, vol. 69, no. 20, pp. 1064–1086, 2021.

[12] X. Deng, Y. Liu, and H. Chen, "Three-dimensional image reconstruction based on improved U-net network for anatomy of pulmonary segmentectomy," *Mathematical Biosciences and Engineering*, vol. 18, no. 4, pp. 3313–3322, 2021.

[13] J. Han, J. Zhang, and Y. Zhao, "Non-textured objects visual SLAM using pola-rization 3D reconstruction," *Array*, vol. 10, no. 2, pp. 100–126, 2021.

[14] J. Huo and X. Yu, "Three-dimensional mechanical parts reconstruction technology based on two-dimensional image," *International Journal of Advanced Robotic Systems*, vol. 17, no. 2, pp. 36–46, 2020.

[15] S. Jiang and K. Wang, "Image Processing and Splicing Method For 3D optical scanning surface reconstruction of wood grain," *International Journal of Pattern Recognition and Artificial Intelligence*, vol. 34, no. 6, pp. 55–69, 2019.

[16] C. Liu, C. A. Shaheed, C. G. Maher, A. J. McLachlan, J. Latimer, and C. C. Lin, "Response to comment by b," *European Journal of Pain*, vol. 24, no. 6, pp. 1209-1210, 2020.

[17] J. Peng, K. Fu, Q. Wei, Y. Qin, and Q. He, "Improved multiview decomposition for single-image high-resolution 3D object reconstruction," *Wireless Communications and Mobile Computing*, vol. 30, no. 20, pp. 102–123, 2020.

[18] F. M. Shah, T. Gaggero, M. Gaiotti, and C. M. Rizzo, "Condition assessment of ship structure using robot assisted 3D-reconstruction," *Ship Technology Research*, vol. 20, no. 9, pp. 1–18, 2021.

[19] J. Shen, S. Meng, M. Ye, W. Yang, and Z. Liu, "3D image reconstruction using an ECT sensor with a single layer of

electrodes," *Measurement Science and Technology*, vol. 52, no. 16, pp. 30–42, 2020.
[20] L. Si, G. Jiang, X. Hu, and B. Liu, "Retina 3D perception reconstruction algorithm based on visual light field image," *IEEE Access*, vol. 8, no. 20, pp. 1904–1912, 2020.
[21] Y. Su, "3D scene reconstruction method based on image optical flow feedback," *International Journal of Information and Communication Technology*, vol. 19, no. 2, pp. 184–201, 2021.
[22] Y. Sun, X. Zhang, and M. Jian, "3D reconstruction of human face from an input image under random lighting condition," *International Journal of Information and Computer Security*, vol. 10, no. 2/3, pp. 248–260, 2018.
[23] T. Ohashi, Y. Ikegami, and Y. Nakamura, "Synergetic reconstruction from 2D pose and 3D motion for wide-space multi-person video motion capture in the wild," *Image and Vision Computing*, vol. 104, no. 20, pp. 453–476, 2020.
[24] M. Xiao, Z. Sun, X. Shen, L. Shi, and J. Zhang, "Research on 3D reconstruction technology of tool wear area," *Manufacturing Technology*, vol. 19, no. 2, pp. 345–349, 2019.
[25] J. Zhang and C. Zhu, "Approach to 3D face reconstruction through local deep feature alignment," *IET Computer Vision*, vol. 13, no. 2, pp. 213–223, 2019.